Chapter 14

Generation and Storage of Single Photons in Collectively Excited Atomic Ensembles

Bo Zhao and Jian-Wei Pan
Hefei National Laboratory for Physical Sciences at Microscale and Department of Modern Physics, University of Science and Technology of China, Hefei, Anhui, 230026, PR China

Chapter Outline

14.1 INTRODUCTION

Deterministic and storable single-photon sources are of crucial importance to all-optical quantum-information processing. In quantum cryptography, single photons can play a role in establishing unconditional security and high efficiency [1,2]. In linear-optical quantum computation, on-demand and indistinguishable single photons are required to implement measurement-induced quantum logic gates [3,4].

In recent years, different quantum systems have been exploited to realize an on-demand single-photon source, such as quantum dots [5,6], single atoms [7,8], and color centers [9] (see Chapter 14). Such single-emitter-based

Single-Photon Generation and Detection, Volume 45. http://dx.doi.org/10.1016/B978-0-12-387695-9.00014-7

single-photon sources often require a high-finesse cavity to ensure that photons are emitted predominantly into a well-defined single spatial mode. In this chapter, we introduce a different type of single-photon source that consists of many identical single-photon emitters, i.e. the atomic-ensemble-based single-photon source. Due to the collective enhancement, these sources can be implemented without the use of high-finesse cavity [10]. Moreover, because the process is reversible, atomic ensembles can also provide storage for single photons due to the inherent bandwidth matching. Controllable transfer of quantum states between a flying qubit and a memory is of crucial importance to quantum-information science [11,12]. Therefore, atomic-ensemble-based single-photon sources present a valuable resource for optical quantum-information processing.

The principle of the atomic-ensemble-based single-photon source may be understood as follows [10,13]. Consider an ensemble of three-level atoms in a lambda configuration initialized with all the atoms in one of the ground states. First, the quantum state of a single photon is imprinted into an atomic ensemble using a "write" process. In this process, a single collective excitation is generated probabilistically in an atomic ensemble via spontaneous Raman scattering by applying a weak coherent write light pulse. The successful generation of the collective excitation is indicated by the detection of a corresponding Raman photon. The collective excitation is then coherently stored in the atomic ensemble, which serves as a quantum memory. In the following "read" process, the single excitation is converted into a single photon by applying a strong coherent read pulse after a controllable delay. The spatial mode, bandwidth, and frequency of the single-photon output are determined by the mode-matching, intensity, and frequency of the retrieval light [13–15].

One distinct advantage of atomic-ensemble-based single-photon sources is that the single photon can be stored in the atomic ensemble and be read out when it is needed. The upper limit of the storage time is determined by the coherence time of the atomic memory, which can be on the order of seconds [16]. Because of the long coherence time, a series of reset pulses (optical pulses that pump the atoms to the initial ground state) and write pulses can be applied to the ensemble. The reset and write pulse sequence is stopped by a feedback circuit, once an anti-Stokes photon is detected. In this way, a collective excitation can be stored in the atomic ensemble, subject to a deterministic readout, and thus a deterministic single-photon source can be implemented [17,18]. The same medium can be used as memory that stores single photons [14,15,19,20].

In this chapter we discuss atomic-ensemble-based single-photon sources. In Section 14.2, we introduce the basic concepts of the write and read processes. In Section 14.3, we show how a heralded single-photon source can be converted into a deterministic one. In Section 14.4, we discuss the indistinguishability of single photons generated from independent sources by examining two-photon Hong-Ou-Mandel interference. We conclude with a brief look into the future.

14.2 BASIC CONCEPTS

Let us first consider a Λ-type three-level atomic system. The energy level structure is depicted in Fig. 14.1, where the upper state $|e\rangle$ is the excited state and two lower states $|a\rangle$ and $|b\rangle$ are the ground states used to store the quantum state. Initially all atoms are prepared in one of the ground states, e.g. $|a\rangle$, by optical pumping. In the write process, an off-resonant weak classical laser pulse coupling $|e\rangle$ and $|a\rangle$ is applied to the atomic ensemble. A small number of atoms will be excited to $|e\rangle$ and almost immediately decay. These atoms that decay into $|b\rangle$ emit anti-Stokes photons; this effect is called spontaneous Raman scattering. According to energy conservation, the number of atoms transferred to the $|b\rangle$ state is equal to the number of anti-Stokes photons emitted from the atomic ensemble. If the write pulse is so weak that only one anti-Stokes photon is generated in the mode of interest, then only one atom changes its state, but it is impossible to know which one, even in principle. The excitation rate must be low so that the probability that more than one photon is created is negligible. In this case, if a single anti-Stokes photon is detected, the atomic ensemble is projected into an equally weighted superposition state, a collective excited state, which can be described by

$$|1\rangle_a = S^\dagger|0\rangle_a = \frac{1}{\sqrt{N}}\sum e^{i\boldsymbol{k}\cdot\boldsymbol{r}_i}|a\ldots b_i\ldots a\rangle, \tag{14.1}$$

where $S^\dagger = \frac{1}{\sqrt{N}}\sum_{i=1}^{N} e^{i\boldsymbol{k}\cdot\boldsymbol{r}_i}|b\rangle_i\langle a|$ is the creation operator of the collective state and $|0\rangle_a = \otimes_i|a\rangle_i$ denotes the atomic vacuum state (see details in Appendix). That is to say, in the write process a quantum state is imprinted into the collective excited state of the atomic ensemble conditional on detecting an anti-Stokes

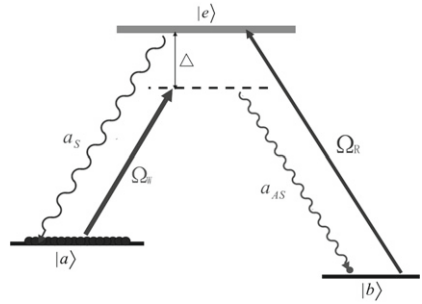

FIGURE 14.1 An illustration of the interaction between the atomic ensemble and light. The excited state $|e\rangle$ and two ground states $|a\rangle$ and $|b\rangle$ form the Λ-type three-level atom. In the write process, an off-resonant write light pulse with Rabi frequency Ω_W and detuning Δ is applied to the atomic ensemble. An anti-Stokes photon is emitted and simultaneously a collective excitation is generated due to spontaneous Raman scattering. In the EIT-based read process, an on-resonance read light pulse with Rabi frequency Ω_R is applied to convert the collective excitation to a Stokes photon.

photon. It should be noted that the two ground states are immune to spontaneous emission, and decoherence of the ensemble as a whole occurs with the rate of a single-atom decoherence.

The collective excitation can be converted into a single photon in the read process. In this process, a strong coherent light pulse, coupling $|e\rangle$ and $|b\rangle$, transfers the collective excitation into a Stokes photon. Since the Stokes photon and the strong read light pulse satisfy the electromagnetically induced transparency (EIT) condition [14,15,19,20], the Stokes photon can propagate through the atomic ensemble with little to no absorption. In the ideal case the excitation stored in the atomic ensemble can be deterministically retrieved (see details in Appendix).

After the write process, the atom-photon state can be described by a two mode squeezed state $|\psi\rangle_{a,\mathrm{AS}} = |0\rangle_a|0\rangle_{\mathrm{AS}} + \sqrt{\chi}|1\rangle_a|1\rangle_{\mathrm{AS}} + \chi|2\rangle_a|2\rangle_{\mathrm{AS}} + O\left(\chi^{\frac{3}{2}}\right)$, where the excitation probability $\chi \ll 1$. After the read process, the collective excitation is converted into a Stokes photon, and thus the photonic state can be described by $|\psi\rangle_{\mathrm{AS,S}} = |0\rangle_{\mathrm{AS}}|0\rangle_{\mathrm{S}} + \sqrt{\chi}|1\rangle_{\mathrm{AS}}|1\rangle_{\mathrm{S}} + \chi|2\rangle_{\mathrm{AS}}|2\rangle_{\mathrm{S}} + O\left(\chi^{\frac{3}{2}}\right)$. The Stokes photon and anti-Stokes photon are non-classically correlated, which leads to a violation of the Cauchy-Schwarz inequality $(g^{(2)}_{\mathrm{AS,S}})^2 \leq g^{(2)}_{\mathrm{AS,AS}} g^{(2)}_{\mathrm{S,S}}$, where $g^{(2)}_{\mathrm{AS,S}}$ is the second-order cross-correlation function, and $g^{(2)}_{\mathrm{S,S}}$ and $g^{(2)}_{\mathrm{AS,AS}}$ are the second-order auto-correlation functions [21]. A straightforward calculation shows $g^{(2)}_{\mathrm{AS,S}} = 1 + 1/\chi$ and $g^{(2)}_{\mathrm{AS,AS}} = g^{(2)}_{\mathrm{S,S}} = 2$. Since $\chi \ll 1$, the Cauchy-Schwarz inequality is violated and the anti-Stokes and Stokes photons are non-classically correlated.

The non-classical correlation between anti-Stokes and Stokes photons allows the preparation of a heralded single-photon source [13–15], in which a single photon can be generated on demand if it is known that there is a collective excitation in the atomic ensemble. The presence of the latter is heralded by the detection of a spontaneous Raman photon in the write process, after which the excitation can be converted into a photon on request. The quality of the heralded single photons can be estimated as follows. Conditional on the detection of an anti-Stokes photon, the Stokes photon may be described by a mixed state $\rho_S = |1\rangle_S\langle 1| + 2\chi|2\rangle_S\langle 2|$. This means the triggered Stokes photon is in a single-photon state that is mixed with a small two-photon component. The normalized auto-correlation of the triggered single photon is $\alpha = \frac{2P_{\mathrm{II}}}{P_{\mathrm{I}}^2} = 4\chi$, where $P_{\mathrm{I}}(P_{\mathrm{II}})$ is the probability of generating one (two) photon(s) per trial (the higher orders are negligible small). For a coherent laser source, $\alpha = 1$, and for an ideal single-photon source $\alpha = 0$. It can be readily seen $\alpha \to 0$ if $\chi \to 0$. Therefore, to obtain a high-quality triggered single photon, the excitation probability must be small. This process is similar to a four-wave-mixing-based single-photon generation (see Chapter 13), but here the "heralded" single photon is stored as an atomic excitation, and its retrieval is a deterministic process. A typical operation of the source would require multiple write attempts, and one read

attempt. This source has a number of advantages common to deterministic sources, particularly, it is scalable.

Atomic-ensemble-based single-photon sources have been demonstrated experimentally both in laser-cooled ensembles [13,14,17] and thermal atomic vapors [15]. The cold atomic ensemble has the advantage of higher single-photon quality and longer coherence time; the following discussion focuses on experiments with cold atomic ensembles.

14.3 FROM HERALDED TO DETERMINISTIC SINGLE-PHOTON SOURCES

Heralded single-photon sources are probabilistic. This significantly limits the usefulness of these sources in scalable all-optical quantum-information processing. Thanks to the storable nature of atomic-ensemble-based single-photon sources, it is possible to implement deterministic single-photon sources by means of a feedback circuit. The basic idea is that a single collective excitation is generated in an atomic ensemble by applying a series of subsequent reset and write pulses. The successful generation of a collective excitation is indicated by the detection of a corresponding anti-Stokes Raman photon. This detection is used as a feedback to stop the sequence and to start the next process, i.e. to convert the excitation back into a single photon after a controllable delay. Such a sequence can be taken as a feedforward operation for the deterministic creation of a single photon. In this way, a deterministic single-photon source is obtained. This controllable deterministic single-photon source potentially paves the way for the construction of scalable quantum communication networks and linear-optical quantum circuits. As one example, we present a proof-of-principle demonstration of a deterministic and storable single-photon source [17]. The single-photon quality is preserved while the production rate of single photons is considerably improved by the aid of the repetitive write process and feedback control.

A schematic of the experimental setup used to demonstrate a deterministic single-photon source is shown in Fig. 14.2a. Cold atoms with a Λ-type three-level configuration (two ground states $|a\rangle$, $|b\rangle$ and an excited state $|e\rangle$) collected by a magneto-optical trap (MOT) [22] are used as the medium for quantum memory. In this experiment, more than 10^8 ^{87}Rb atoms are collected by the MOT with an optical depth of about 5 and have a temperature of about 100 μK. To prevent Zeeman splitting, the earth's magnetic field is compensated by three pairs of Helmholtz coils. The two ground states $|a\rangle$, $|b\rangle$ and the excited state $|e\rangle$ are the $|5S_{1/2}, F = 2\rangle$, $|5S_{1/2}, F = 1\rangle$, and $|5P_{1/2}, F = 2\rangle$ states of ^{87}Rb, respectively. The write laser is tuned to the transition from $|5S_{1/2}, F = 2\rangle$ to $|5P_{1/2}, F = 2\rangle$ with a detuning of 10 MHz, and the read laser is locked on-resonance to the transition from $|5S_{1/2}, F = 1\rangle$ to $|5P_{1/2}, F = 2\rangle$. The write and read beams have orthogonal polarizations, and are spatially overlapped

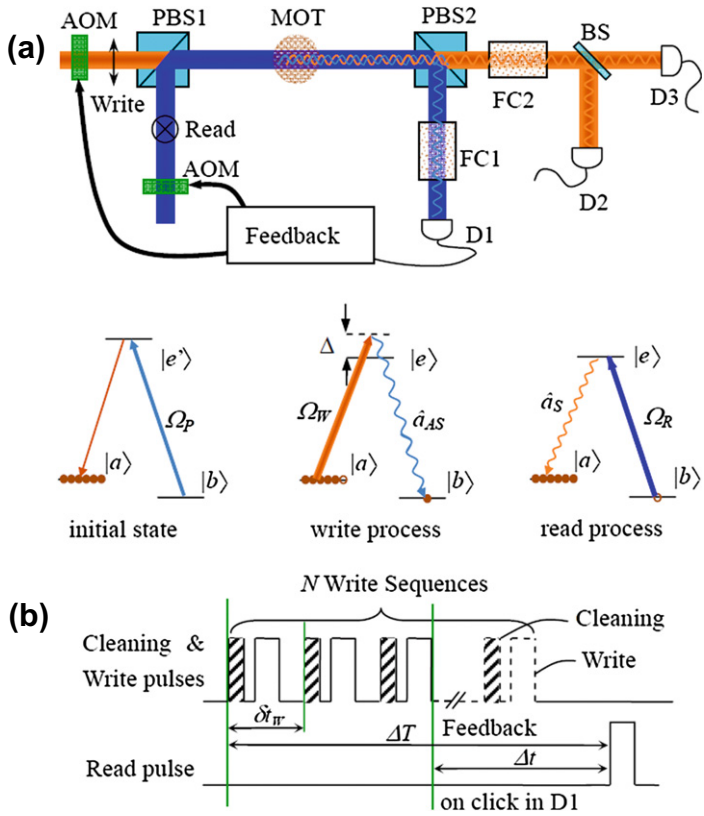

FIGURE 14.2 (a) Illustration of the experimental setup and (b) the time sequence with the feedback circuit for the write and read processes. The atomic ensemble is first prepared in the initial state $|a\rangle$ by applying a reset (cleaning) pump beam resonant with the transition $|b\rangle$ to $|e'\rangle$. A write pulse with the Rabi frequency Ω_W is applied to generate the spin excitation and an accompanying photon of the mode $\hat{a}_{\rm AS}$. After a delay Δt, a read pulse is applied with orthogonal polarization and it spatially overlaps with the write beam in PBS1. The photons, whose polarization is orthogonal to that of the write beam, in the mode $\hat{a}_{\rm AS}$ are extracted from the classical write beam by PBS2 and detected by detector D1. Similarly, the field $\hat{a}_S$ is extracted from the Read beam and detected by detector D2 (or D3). Here, FC1 and FC2 are two filter cells, BS is a 50/50 non-polarizing beam splitter, and AOM1 and AOM2 are two acousto-optic modulators.

on a polarizing beam splitter (PBS1), and then focused into the cold atoms with a beam waist of 35 μm. After passing through the atomic cloud, another polarizing beam splitter (PBS2) separates the classical write (read) beam from the generated anti-Stokes (Stokes) field, and cells filled with ^{87}Rb atoms prepared in state $|5S_{1/2}, F = 2\rangle$ $\left(|5S_{1/2}, F = 1\rangle\right)$ are used to further suppress the residual light from the read/write pulses.

After switching off both the MOT optical beams and magnetic field, the atoms are first optically pumped to the initial state $|a\rangle$ by a reset pulse. Then

a classical write pulse ($\approx 10^4$ photons) with a duration of 100 ns is applied onto the atomic ensemble to produce, via the spontaneous Raman transition $|a\rangle \rightarrow |e\rangle \rightarrow |b\rangle$, a superposition state of the anti-Stokes field and the collective spin, $|\psi\rangle_{a,\mathrm{AS}} = |0\rangle_a|0\rangle_{\mathrm{AS}} + \sqrt{\chi}|1\rangle_a|1\rangle_{\mathrm{AS}} + \chi|2\rangle_a|2\rangle_{\mathrm{AS}} + O\left(\chi^{\frac{3}{2}}\right)$ with a probability of $\chi \ll 1$. After a controllable delay δt, a read pulse with a duration of 75 ns is applied to convert the collective excitation into the Stokes field. The intensity of the read pulse is about 100 times stronger than that of the write pulse.

The cross-correlation between the Stokes and anti-Stokes photons is defined as $g^{(2)}_{\mathrm{S,AS}} = \frac{p_{\mathrm{S,AS}}}{p_{\mathrm{S}} p_{\mathrm{AS}}}$, where $p_{\mathrm{S,AS}} = \chi \eta_{\mathrm{ret}} \eta_{\mathrm{AS}} \eta_{\mathrm{S}}$ is the coincidence probability, η_{ret} is the retrieval efficiency, and $\eta_{\mathrm{S}}\left(\eta_{\mathrm{AS}}\right)$ is the overall detection efficiency of the Stokes (anti-Stokes) channel (including the transmission efficiency of filters and optical components, the coupling efficiency of the fiber couplers, and the detection efficiency of single-photon detectors), and $p_{\mathrm{S}} = \chi \eta_{\mathrm{ret}} \eta_{\mathrm{S}}\left(p_{\mathrm{AS}} = \chi \eta_{\mathrm{AS}}\right)$ is the probability of detecting a Stokes (anti-Stokes) photon. The anti-Stokes photon is registered by the single-photon detector D1, and the retrieved Stokes photon is registered by detectors D2 and D3. The cross-correlation as a function of p_{AS} is shown in Fig. 14.3a, which clearly demonstrates that the cross-correlation is inversely proportional to the excitation probability. The cross-correlation versus storage time is shown in Fig. 14.3b, which gives a coherence time of the quantum memory of about 12 μs for this implementation. A coherence time of a few tens of microseconds is mainly caused by the residual magnetic field [23].

The single-photon quality is characterized by the conditional auto-correlation of the Stokes photons $\alpha = \frac{p_{(23|\mathrm{AS})}}{p_{(2|\mathrm{AS})} p_{(3|\mathrm{AS})}}$ [24], where $p_{(23|\mathrm{AS})}$ is the coincident probability between single-photon detectors D2 and D3 conditioned on the detection of an anti-Stokes photon on D1, and $p_{(2|\mathrm{AS})}(p_{(3|\mathrm{AS})})$ is the conditional probability on D2 (D3). Figure 14.4a shows α as a function of excitation probability. For small χ, $\alpha = 4\chi$ [13]. $\alpha < 1$ indicates that the triggered Stokes photon approximates a single-photon state. We note that, for $p_{\mathrm{AS}} \rightarrow 0, \alpha = 0.057(28)$, which deviates from the ideal value of 0. This offset comes from noise, including the residual leakage of the write and read beams, stray light, and the dark counts of the detectors.

To make a deterministic single-photon source, a number of write pulses per experimental trial and the feedback protocol are applied as discussed above. A realistic time sequence is shown in Fig. 14.2b. In the time interval ΔT, N independent write sequences with a period of δt_W are applied to the atomic ensemble. Each write sequence contains a reset pulse and a write pulse. Once an anti-Stokes photon is detected by D1, the feedback circuit stops further write sequences and enables the read pulse to retrieve the single Stokes photon after a programmable delay Δt. The maximum number of write sequences is determined by the ratio of δt_W and the coherence time of the quantum memory. The feedback protocol enhances the production probability of

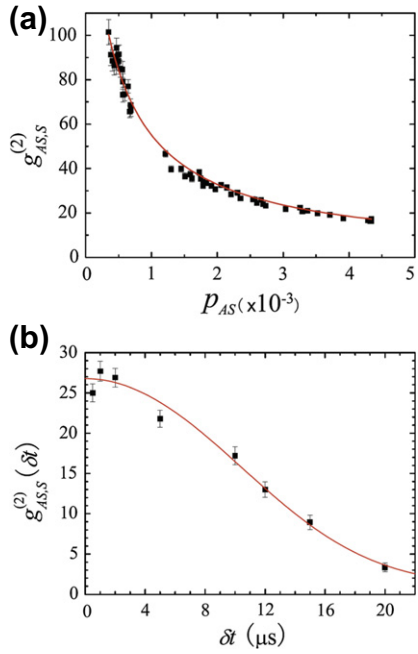

FIGURE 14.3 Intensity correlation functions $g^{(2)}_{\mathrm{S,AS}}$ along the excitation probability p_{AS} with $\delta t = 500$ ns (a) and along the time delay δt between read and write pulses with $p_{\mathrm{AS}} = 3 \times 10^{-3}$ (b). The observed lifetime is $\tau_C = 12.5 \pm 2.6$ μs.

anti-Stokes photons according to the new excitation probability

$$P_{\mathrm{tot}} = \sum_{j=1}^{N} p_{\mathrm{AS}}(1 - p_{\mathrm{AS}})^{j-1}. \tag{14.2}$$

And the conditional probability is

$$P_{\mathrm{i/AS}} = \sum_{j=0}^{N-1} p_{\mathrm{AS}},(1 - p_{\mathrm{AS}})^{j-1} p_{\mathrm{i/AS},(\Delta T - j\delta t_W)}, \tag{14.3}$$

with $i = 2$, 3 and 23. $p_{\mathrm{i/AS},(\Delta T - j\delta t_W)}$ is the conditional detection probability after applying the jth write pulse. In this setup, the normalized auto-correlation function is given by $\alpha = \frac{P_{(23|\mathrm{AS})}}{P_{(2|\mathrm{AS})} P_{(3|\mathrm{AS})}}$. This protocol can be executed in different modes. In the first mode, one can fix the retrieve time ΔT. Therefore, the delay Δt varies because the spin excitation is created randomly by one of the write sequences. Single photons are produced at a given time with a high probability, approaching unity if $N \gg 1$. In the second mode, we retrieve the single photons with a fixed delay Δt after a successful write process. In this case, the imprinted

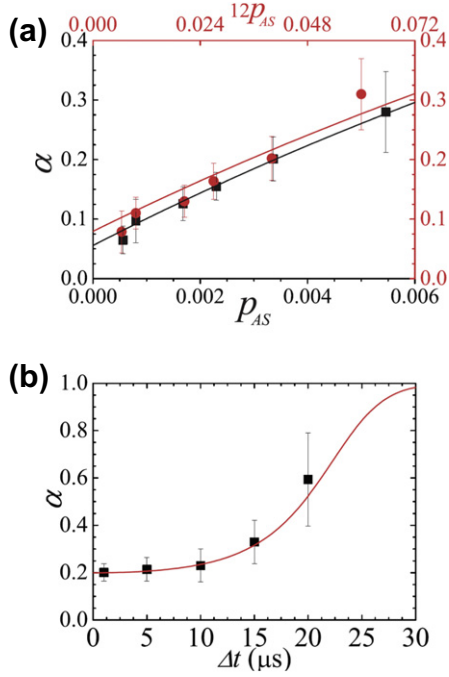

FIGURE 14.4 The auto-correlation parameter as a function of p_{AS} (a) and δt (b). In panel (a), the data in black (square dots) corresponds to the experiment without feedback circuit, in which each write sequence is followed by one read pulse. The data in gray (circular dots) corresponds to the experiment with feedback circuit, in which 12 successive write sequences are followed by one read pulse. The gray curve (upper curve) is the theoretical evaluation taking into account the fitted background of the black dots. In panel (b), 12 write sequences were applied in each trial while measuring.

single excitation can be converted into a single photon at any given time within the coherence time of the quantum memory. The first mode can serve as a deterministic single-photon source and is well suited for all-optical quantum information processing.

In the experiment, $\Delta T = 12.5$ μs and $\delta t_W = 1$ μs, i.e. up to 12 write sequences can be used. The measured auto-correlation parameter α is shown in Fig. 14.4a as a function of the excitation probability p_{AS}. For $N = 1$, α is nearly linear for $p_{AS} \leq 0.006$. For $N = 12$ successive write sequences, α is plotted versus $12p_{\mathrm{AS}}$. Compared with $N = 1$ we can easily see that α is preserved, and the excitation probability is enhanced by the repetitive write sequences. If the coherence time of the spin excitation is long enough to allow many write sequences, the excitation probability can reach unity while preserving the single-photon nature of the output. In this case, the generation efficiency depends only on the retrieval efficiency. In the second experiment, we fix $\delta t_W = 1$ μs and $N = 12$. Figure 14.4b shows the measured as a function

of Δt. For each Δt, ΔT varies due to the random creation of the collective excitation by the N write sequences. Again, it is clear that the single-photon nature is well preserved within the coherence time of the quantum memory.

The production rate of the single photons is determined by the coherence time of the quantum memory, the retrieval efficiency, and the duration of the pulses. To enhance the production rate, it is necessary to improve both the coherence time of the quantum memory and the retrieval efficiency. Moreover, by further improving the control circuit, i.e. reducing the period of write pulses due to electronic delays, more write pulses can be applied within the lifetime. A simple estimation shows that with $p_{AS} \sim 0.003$ and a write period of 300 ns, we may obtain a single-photon source with a probability as high as 95% within a coherence time of 300 μs.

14.4 INTERFERENCE OF PHOTONS FROM INDEPENDENT SOURCES

In the linear-optical quantum computing protocol proposed by Knill *et al.* [3], single photons from independent sources interact in a Mach-Zehnder-like interferometer and a single-photon detection is used to implement a controlled phase gate. In the polarization-entanglement-based scheme proposed by Browne *et al.* [4], two photons from independent sources are sent to a Hong-Ou-Mandel (HOM) type interferometer [25] to implement coalescence gates [4]. In both cases, a unity visibility can be achieved only if the photons are indistinguishable [26,27].

The indistinguishability of single photons has been examined in recent years [28–30]. In this section, we show that the two photons generated from two independent atomic ensembles are pure and indistinguishable, as indicated by the high two-photon HOM interference visibility. The two indistinguishable single photons can also be used to generate polarization entanglement by post-selection.

The experimental setup is depicted in Fig. 14.5. Atomic ensembles collected by two MOTs that are 0.6 m apart serve as the media for quantum memories and deterministic single-photon sources. The atomic system is the same as the one described in Section 15.3. A write pulse that generates the collective excitation is detuned by 10 MHz and loosely focused to a beam diameter of about 400 μm through the atomic ensemble in the MOT. The emitted anti-Stokes photon is collected into a single-mode optical fiber with the mode diameter of about 100 μm in the interaction region. The optical axis of the anti-Stokes field is tilted by 3° [31] from that of the write beam. As described above, the detection of a single anti-Stokes photon heralds a single collective excitation in the atomic ensemble with complete certainty. After a controllable time delay, a classical read pulse with an orthogonal polarization and spatially mode-matched with the

write beam is applied from the opposite direction. The collective excitation in the atomic ensemble is converted into a single-photon excitation in the Stokes field, which propagates in the opposite direction of the anti-Stokes field and is collected into a single-mode fiber. If the retrieval efficiency is unity, the emission of the single Stokes photon is deterministic. Changing from the co-propagating configuration described in the last section to a counter-propagating configuration, and tilting the Stokes and anti-Stokes modes by 3° relative to the classical write and read beams, are convenient ways to separate the quantum fields from the intense classical light.

As shown in Fig. 14.5b, Alice and Bob have similar sources. They each prepare collective spin excitations independently and whichever one finishes the preparation first waits for the other while keeping the collective spin excitation in her/his quantum memory. After both Alice and Bob have finished their preparations, they retrieve the excitations simultaneously at any time within the coherence time of the collective state. Therefore the retrieved photons arrive at the beam splitter contemporarily. The coherence time of the single photons is adjustable and is set to be about 25 ns in this demonstration. This long coherence time is chosen to reduce the impact of a possible small temporal mismatch between Alice and Bob that can arise from the optical path difference. Note that the read and write lasers used for different single-photon sources are completely independent of each other. This guarantees there is no spatial-temporal correlation between the single photons [32].

Compared to a probabilistic photon source, deterministic sources based on atomic ensembles achieve a considerable enhancement of the coincidence rate of single photons coming from Alice and Bob. For instance, consider a probabilistic version of the same experimental setup, in which Alice and Bob operate without the feedback circuit, and instead apply a write pulse and a read pulse in every experimental trial and monitor fourfold coincidences between the anti-Stokes and Stokes photons in the four channels D1, D2, C1, and C2. Assuming that the probability of having an anti-Stokes photon in channel D1 (D2) is p_{AS1} (p_{AS2}), and the corresponding retrieval efficiency of converting the spin excitation to a Stokes photon coupled into channel C1 (C2) is $\eta_{\mathrm{ret1}}(\delta t_{\mathrm{R}})$, the probability of fourfold coincidence is $p_{4\mathrm{c}} = p_{\mathrm{AS1}}\eta_{\mathrm{ret1}}(\delta t_{\mathrm{R}})p_{\mathrm{AS2}}\eta_{\mathrm{ret2}}(\delta t_{\mathrm{R}})$. This can be compared to the feedback-circuit based scheme shown in Fig. 14.5b, where we can apply N write pulses in each trial. Assuming $p_{\mathrm{AS1}}, p_{\mathrm{AS2}} \ll 1$, the probability of fourfold coincidence can be approximated as $p_{4\mathrm{c}} \approx N^2 p_{\mathrm{AS1}}\eta_{\mathrm{ret1}}(\delta t_{\mathrm{R}})p_{\mathrm{AS2}}\eta_{\mathrm{ret2}}(\delta t_{\mathrm{R}})$, which shows that the probability of fourfold coincidence is enhanced by N^2 for each trial. For this demonstration, $p_{\mathrm{AS1}} = p_{\mathrm{AS2}} \approx 0.002$ (the corresponding cross-correlation $g^{(2)}_{\mathrm{S,AS}} = 30$), $N = 12$, $\tau_{\mathrm{C}} \approx 12\ \mu s$, $\delta t_{\mathrm{R}} = 400$ ns, and $\eta_{\mathrm{ret1}}(0) = \eta_{\mathrm{ret2}}(0) \approx 8\%$.

The four lasers in Fig. 14.5b are independently frequency-stabilized. The full width at half maximum (FWHM) linewidths of W1 and R1 are about 1 MHz while those of W2 and R2 are about 5 MHz). They are broadened to more than

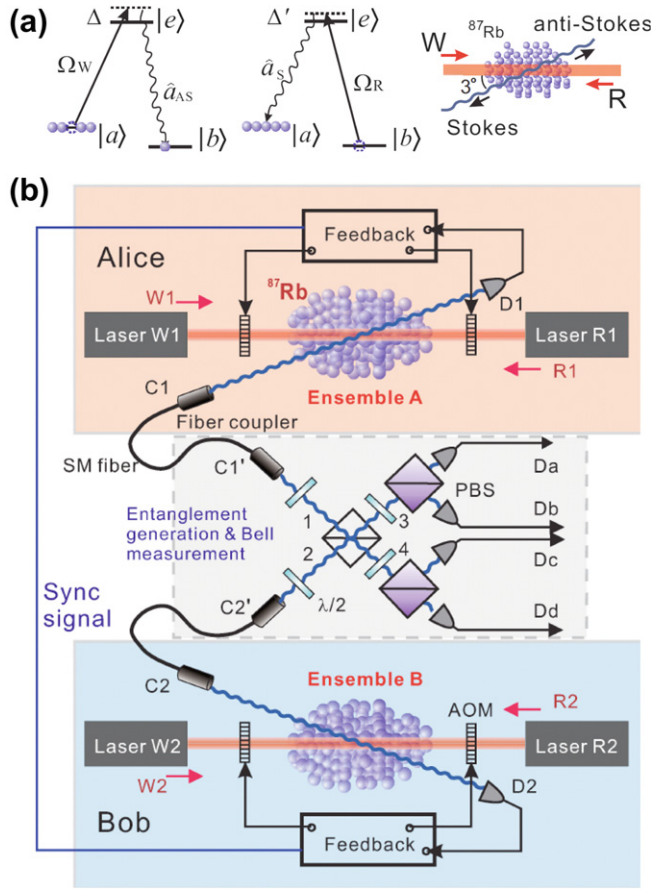

FIGURE 14.5 Illustration of the relevant energy levels of the atoms and arrangement of laser beams (a) and the experimental setup (b). Alice and Bob both keep a single-photon source at two remote locations. Alice applies write pulses continuously until an anti-Stokes photon is registered by detector D1. Then she stops the write pulse, holds on to the spin excitations, sends a synchronization signal to Bob, and waits for his response (This is realized by the feedback circuit and the acousto-optic modulators, AOM). In parallel, Bob prepares a single excitation in the same way as Alice does. After they both agree that each has a collective excitation stored, both simultaneously apply a read pulse to retrieve the spin excitation into a light field $\hat{a}_S$. The two Stokes photons propagate to the place for entanglement generation and a subsequent Bell measurement. Photons overlap at a 50:50 beam splitter (BS) and then will be analyzed by half-wave plates, polarized beam splitters (PBS), and single-photon detectors Da, Db, Dc, and Dd.

20 MHz because the finite bandwidth of AOM limits the shortest pulse width of 40 ns. The linewidth of the retrieved single photons is determined mainly by the linewidth and intensity of the read lasers. In order to verify that the two Stokes photons coming from Alice and Bob are indistinguishable, we overlap them at a non-polarizing beam splitter with the same polarization (horizontal in this case) and measure the two-photon HOM interference. The visibility of the

HOM interference can be expressed in terms of the purity of the single photons [32] $V = Tr(\rho_{S1}\rho_{S2}) = [P(\rho_{S1}) + P(\rho_{S2}) - O(\rho_{S1},\rho_{S2})]/2$, where $\rho_{S1,S2}$ is the reduced density matrix of Stokes photon 1 and 2, $P(\rho_{Si}) = Tr\left(\rho_{Si}^2\right) \leq 1$ $(i = 1,2)$ is the purity, and $O(\rho_{S1},\rho_{S2}) = \|\rho_{S1} - \rho_{S2}\|^2 \geq 0$ is the operational distance between the states of the two photons. It can be easily seen that the visibility gives a lower bound on the mean purity of the single photons. (See Chapter 2 for further discussions on purity, visibility, and indistinguishability.)

We perform HOM interference measurements in both the time domain and the frequency domain. The polarizations of the anti-Stokes photons were set to horizontal with two half-wave plates before they enter the BS, as shown in Fig. 14.5b. The other two half-wave plates after the BS were set to 0°. In the first measurement, fourfold coincidences between detectors D1, D2, Da, and Dd were monitored while changing the time delay between the two read pulses. The excitation probabilities $p_{AS1} = p_{AS2} \approx 0.002$. The coincidence-rate variation with delay is shown in Fig. 14.6. Ideally, there should be complete destructive interference if the wave packets of the two photons overlap perfectly. However, in practice it is difficult to ensure that the two wave packets are identical and perfectly overlapped. We obtained the visibility $V = \frac{C_{plat} - C_{dip}}{C_{plat}} = 80(1)\%$, where C_{plat} is the measured four-photon coincidence rate at the plateau and C_{dip} the rate at the dip. The asymmetry of the profile at a negative delay versus a positive delay shows that the two wave packets are (a) not perfectly identical, (b) not symmetric themselves. Assuming that the HOM dip possesses a Gaussian-type profile, we verify the coherence time to be 25(1) ns FWHM.

In the second measurement, we measured the fourfold coincidence while changing the relative frequency detuning between the two read pulses (Fig. 14.6b, lower panel). The excitation probabilities are $p_{AS1} = p_{AS2} \approx 0.003$. The frequency detuning varies from −30 MHz to 30 MHz limited by the instruments in use. The coincidence rate at the largest detuning was compared to the coincidence rate when the photons impinge the BS with orthogonal polarizations, and the two rates are consistent with each other, thus confirming that the plateau of the HOM dip has been reached. The measured visibility of 82(3)% agrees well with that obtained in the time-domain measurements. The width of the HOM dip is 35(3) MHz FWHM, in agreement with the coherence time of 25 ns. Therefore, the narrow-band nature of the source is directly verified by the HOM dip in the frequency domain. From the visibility, we estimate that the lower bound on the purity of the single photons is about 0.8.

The visibility may be reduced by the imperfect overlap of the two-photon wave packets. Besides, the imperfection of the single-photon sources affects the visibility as well. As discussed in the last section, the quality of the single-photon source can be characterized by the auto-correlation parameter $\alpha = 2P_{II}/P_I^2$, where $P_I(P_{II})$ is the probability of generating one (two) photon(s) from each source (the higher orders are negligible small). If the two single-photon wave packets do not overlap at all then there is no interference, and we obtain the non-correlated coincidence rate $C_{plat} = \frac{P_I^2}{2} + P_{II}$ between Da and Dd. If they

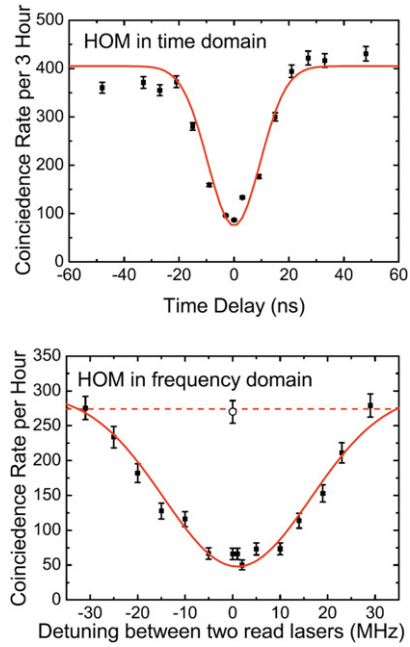

FIGURE 14.6 HOM dips in time domain (upper panel) and frequency domain (lower panel). The open circle in the lower panel was obtained by setting the polarization of the two photons perpendicular to each other and zero detuning between two read lasers, i.e. with fully distinguishable photons. The Gaussian curves that roughly connect the data points are only shown to guide the eye. The dashed line shows the plateau of the dip. Error bars represent statistical errors, which are ± 1 standard deviation.

overlap perfectly, there is a destructive interference leading to a coincidence rate $C_{\text{plat}} = P_{\text{II}}$. So the visibility of the HOM dip is $V = 1/(1+\alpha)$, where $\alpha = 0.12$ for the source prepared later (with the collective excitation retrieved immediately), and 0.17 for the source prepared earlier (it has to wait for the other one). This leads to an average visibility of 87%. In the frequency domain, the average visibility is around 83% because of higher excitation probabilities. In Fig. 14.6, the HOM dip is measured by setting the coincidence window ($\sim$50 ns) larger than the wave-packet length of the single photons ($\sim$25 ns).

Two indistinguishable single photons can be used to generate entanglement by post-selection [33], as illustrated in Fig. 14.5b. Before the BS, half-wave plates set the Stokes photons to orthogonal polarizations (horizontal and vertical). If there is coincidence between output ports 3 and 4, then the state of the two photons will be projected onto a Bell state $|\psi^-\rangle_{12} = \frac{1}{\sqrt{2}}\left(|H\rangle_1|V\rangle_2 - |V\rangle_1|H\rangle_2\right)$. With another two half-wave plates and two PBSs after the BS, the entanglement of the two photons can be verified by a Clauser-Horne-Shimony-Holt (CHSH)-type inequality [34], in which local realism

implies that $S \leq 2$, with $S = |E(\theta_1, \theta_2) - E(\theta_1, \theta_2') + E(\theta_1', \theta_2) + E(\theta_1', \theta_2')|$. Here $E(\theta_1, \theta_2)$ is the correlation function, where θ_1 and θ_1' (θ_2 and θ_2') are the measured polarization angles of the Stokes photon at port 3 (4). We obtain $S = 2.37(0.07)$, which violates the CHSH inequality by 5 standard deviations. Taking into account the two-photon component in the single-photon sources, a straightforward calculation shows the violation of the CHSH inequality is about 2.3, which is in good agreement with the experimental results.

14.5 CONCLUSION AND OUTLOOK

In this chapter, we have introduced the atomic-ensemble-based single-photon sources. The advantages of this type of source are (1) it does not require strong coupling between light and emitters thanks to the collective enhancement; (2) the linewidth of the photons naturally matches that of an atomic memory implemented in the same physical system, making the emitted single photons readily storable; (3) the emitted photons are narrow-band and highly controllable. With the aid of a feedback circuit, this source can approximate a deterministic single-photon source. Being a key device in any scalable quantum communications network, and for large-scale linear-optical computation, this circuit shows a promising enhancement in excitation probability while preserving the single-photon nature of the output. Synchronized generation of narrow-band single photons from two independent atomic ensembles has been demonstrated. The Hong-Ou-Mandel dip was observed in both the time domain and the frequency domain with a high visibility for independent photons from two separate sources, demonstrating the indistinguishability of these photons.

Atomic-ensemble-based single-photon sources hold promise for all-optical scalable quantum-information processing. Recently, remarkable progresses have been achieved toward quantum-information processing with atomic ensembles and linear optics. For example, DLCZ-type entanglement between two atomic ensembles has been created [35], and functional quantum-repeater nodes with atomic ensembles have been demonstrated [36,37]. The storage of single photons has been realized where heralded single photon emitted from one atomic-ensemble-based single-photon source is stored in a remote atomic quantum memory [14,15,38].

To make atomic-ensemble single-photon sources truly useful in practice, the coherence time and the retrieval efficiency must be significantly improved. In the atomic ensemble, the coherence time of the collective state suffers from the residual magnetic field around the MOT. It has been demonstrated that by using magnetic-field-insensitive states to store the collective excitation and suppressing decoherence due to atomic random motion by reducing the angle between write and anti-Stokes mode, or by using a one-dimensional optical lattice to trap the atoms, millisecond quantum memories can be achieved [39–42]. A recent experiment demonstrated a coherent storage time of 16 s

in ultracold atoms for classical states of light [16]. The retrieval efficiency can also be improved, for example, by increasing the optical depth of the atomic ensemble, or by putting the atomic ensemble inside a cavity. Using these techniques a retrieval efficiency of 84 % has been achieved for a storage time of a few hundred nanoseconds [43]. Achieving efficient retrieval and long storage times in a single experiment can be done by combing these two advances, as demonstrated in Ref. [44], where a retrieval efficiency of 73 % and a coherence time of 3 ms are reported.

APPENDIX

A Write Process

Let us consider a pencil-shaped cold atomic ensemble containing N 3-level atoms, with ground states $|a\rangle$, $|b\rangle$ and an excited state $|e\rangle$. We denote the axial direction as z direction and assume the zero point is at the center of the atomic ensemble. Initially, all the atoms are in the ground state $|a\rangle$. The off-resonant classical write pulse coupling the excited state $|e\rangle$ and the ground state $|a\rangle$ is given by $\boldsymbol{E}_W(\boldsymbol{r},t) = \hat{\epsilon}_W E_W(\boldsymbol{r},t)e^{i(\boldsymbol{k}_W\cdot\boldsymbol{r}-\omega_W t)}+\text{h.c.}$, where $\hat{\epsilon}_W$ is the polarization unit vector, $\omega_W = ck_W$ is the angular frequency of the write light. For simplicity, we assume the write light pulse propagating along the axial direction $\boldsymbol{k}_W = k_W\hat{z}$. The anti-Stokes field coupling the excited state $|e\rangle$ and ground state $|b\rangle$ is quantum mechanically described as $\boldsymbol{E}_{AS}(\boldsymbol{r},t) = \sum_{\boldsymbol{k}} \hat{\epsilon}_{\boldsymbol{k}}\varepsilon_{\boldsymbol{k}}\hat{a}_{\boldsymbol{k}}e^{i(\mathbf{k}\cdot\boldsymbol{r}-\omega_{\boldsymbol{k}}t)} + \text{h.c.}$, where $\varepsilon_{\boldsymbol{k}} = \sqrt{\frac{\hbar\omega_{\boldsymbol{k}}}{2\epsilon_0 V}}$, $\omega_{\boldsymbol{k}} = ck$, $\hat{\epsilon}_{\boldsymbol{k}}$ is the polarization unit vector, and $\hat{a}_{\boldsymbol{k}}$ is the annihilation operator of mode $\mathbf{k}$. In the cold atomic ensemble, because of the extremely low temperature and the short pulse length of the write light, we can safely assume the atoms are fixed at certain positions during the write process and denote the coordinate of the ith atom by $\boldsymbol{r}_i$. The total Hamiltonian in the rotating frame is given by

$$H = \sum_{i=1}^{N}\left[\hbar\Delta\sigma_{ee}^{i} - \hbar\Omega_W(\boldsymbol{r}_i,t)e^{i\boldsymbol{k}_W\cdot\boldsymbol{r}_i}\sigma_{ea}^{i} + \sum_{\boldsymbol{k}}\hbar g_{\boldsymbol{k}}\hat{a}_{\boldsymbol{k}}e^{i(\mathbf{k}\cdot\boldsymbol{r}_i-\Delta\omega_{\boldsymbol{k}}t)}\sigma_{eb}^{i} + \text{h. c.}\right], \tag{A.1}$$

where the detuning $\Delta = \omega_{ea} - \omega_W$ and $\Delta\omega_{\boldsymbol{k}} = \omega_{\boldsymbol{k}} - \omega_W - \omega_{ba}$, with $\omega_{ea} = \omega_e - \omega_a$ and $\omega_{ba} = \omega_b - \omega_a$ the difference between atomic levels. The spin operators of $\sigma_{lm}^{i} = |l\rangle_i\langle m|$ $\left(l,m = e,a,b\right)$ are the transition operators of ith atom, $\Omega_W\left(\boldsymbol{r},t\right) = \frac{\boldsymbol{d}_{ea}\cdot\hat{\epsilon}_W E_W(\boldsymbol{r},t)}{\hbar}$ with $\boldsymbol{d}_{ea} = \langle e|\boldsymbol{d}|a\rangle$ being the Rabi frequency of the write light, and $g_{\boldsymbol{k}} = -\frac{\boldsymbol{d}_{eb}\cdot\hat{\epsilon}_{\boldsymbol{k}}\varepsilon_{\boldsymbol{k}}}{\hbar}$ with $\boldsymbol{d}_{eb} = \langle e|\boldsymbol{d}|b\rangle$ is the coupling coefficient of each mode of the anti-Stokes light.

If the Rabi frequency of the write light and the linewidth of the excited state are both significantly smaller than the detuning Δ, the upper state $|e\rangle$ can be adiabatically eliminated, and each atom is described by an effective two-level

model. The resulting adiabatic Hamiltonian is given by

$$H = \sum_{i=1}^{N}\left[\frac{\Omega_W(\boldsymbol{r}_i,t)}{\Delta}e^{i\boldsymbol{k}_W\cdot\boldsymbol{r}_i}\sigma_{ba}^{i}\sum_{\boldsymbol{k}}\hbar g_{\boldsymbol{k}}\hat{a}_{\boldsymbol{k}}^{\dagger}e^{-i(\boldsymbol{k}\cdot\boldsymbol{r}_i-\Delta\omega_{\boldsymbol{k}}t)} + \text{h. c.}\right], \tag{A.2}$$

where we have neglected the small AC Stark shift. This adiabatic Hamiltonian describes the spontaneous emission of N atoms from the pseudo excited state $|a\rangle$ to the pseudo ground state $|b\rangle$ where the frequency of the emitted anti-Stokes light is centered at $\omega_S = \omega_W - \omega_{ba}$. The linewidth of the pseudo excited state is $\Gamma' = \frac{\Omega_W^2}{\Delta^2}\Gamma$, with Γ the decay rate from $|e\rangle$ to $|b\rangle$. This Hamiltonian has been extensively investigated in last two decades [45]. The initial stage can be well described by spontaneous emission where the anti-Stokes photon is emitted along all the directions. After a time $1/\Gamma'$, the anti-Stokes light will dominate along the axial direction and enter the superradiance regime. In our case, the interaction time T is determined by the pulse duration of the write beam which is short compared to the lifetime $1/\Gamma'$, and thus we are in the spontaneous emission regime. Therefore we can simply solve the Schrödinger equation by using perturbation theory. To the first order of the perturbation, the atom-light system is described by

$$|\psi\rangle = \left[1 - i\int_0^T H(\tau)\,d\tau\right]|\text{vac}\rangle + o(p) \tag{A.3}$$

with $|\text{vac}\rangle = |0\rangle_a|0\rangle_p$, where $|0\rangle_a = \otimes_i|a\rangle_i$ the atomic vacuum state and is $|0\rangle_p$ the light vacuum. Integrating out τ, we obtain

$$|\psi\rangle = |0\rangle_a|0\rangle_p + \sum_{i}^{N}\frac{\Omega_W(\boldsymbol{r}_i)}{\Delta}e^{i\boldsymbol{k}_W\cdot\boldsymbol{r}_i}|a\ldots b_i\ldots a\rangle|\gamma\rangle_i, \tag{A.4}$$

where $|\gamma\rangle_i = -i\int_0^T\sum_{\boldsymbol{k}} g_{\boldsymbol{k}}a_{\boldsymbol{k}}^{\dagger}e^{-i(\boldsymbol{k}\cdot\boldsymbol{r}_i-\Delta\omega_{\boldsymbol{k}}t)}|0\rangle_p$ is the spontaneously emitted anti-Stokes light from the ith atom, and we have assumed the Rabi frequency is time independent. It can be easily seen that in the spontaneous emission regime the atoms emit anti-Stokes photons into all the directions independently from each other.

As discussed in standard quantum optics textbooks [46], the spatial wave function of the photon emitted from ith atom can be described by $E_i(\Delta r_i) = \frac{\varepsilon_0}{\Delta r_i}e^{ik_{AS}\Delta r_i}$ where $k_{AS} = \frac{\omega_{AS}}{c}$, ε_0 is the constant proportional to the electro-dipole transition matrix element, $\Delta r_i = |\boldsymbol{r} - \boldsymbol{r}_i|$ is the distance between the ith atom and observation point $\boldsymbol{r}$. Assume we observe the anti-Stokes light along the axial direction, i.e. z direction, under the paraxial axial approximation $|\text{z} - \text{z}_i| \gg x^2, y^2, x_i^2, y_i^2$, the wave function on the observation surface may be

expressed as

$$
\begin{aligned}
E_i(\boldsymbol{r}) = & \frac{\varepsilon_0}{z-z_i}\exp\left[ik_{\mathrm{AS}}\left(z-z_i+\frac{x_i^2+y_i^2}{2(z-z_i)}+\frac{x^2+y^2}{2(z-z_i)}\right)\right. \\
& \left.-ik_{\mathrm{AS}}\frac{x_i x+y_i y}{z-z_i}\right] \\
\approx & \frac{\varepsilon_0}{z}\exp(-ik_{\mathrm{AS}}z_i)\exp\left[ik_{\mathrm{AS}}\left(z+\frac{x_i^2+y_i^2}{2z}\right.\right. \\
& \left.\left.+\frac{x^2+y^2}{2z}-\frac{x_i x+y_i y}{z}\right)\right] \\
& \times\exp\left[ik_{\mathrm{AS}}\left(\frac{x_i^2+y_i^2}{2z^2}z_i+\frac{x^2+y^2}{2z^2}z_i\right.\right. \\
& \left.\left.-\frac{x_i x+y_i y}{z^2}z_i\right)\right],
\end{aligned}
\tag{A.5}
$$

where $|z_i| \ll z$ is assumed. We define two diffraction angles with $\theta_{W_a} = \frac{1}{k_{\mathrm{AS}} W_a}$ and $\theta_{\mathrm{L}} = \left(\frac{1}{k_{\mathrm{AS}} L}\right)^{1/2}$, where W_a and L are the waist and length of the atomic ensemble, respectively. It can be readily seen that if the detection angle $\theta \leq \min(\theta_{W_a}, \theta_L)$, all the phase factors which are related to coordinates of the atoms, except $\exp(-\mathrm{i}k_{AS}z_i)$, can be safely neglected. Thus the anti-Stokes light on the observation surface can be treated as a single mode and the spatial wave function may be described by $E_i(\boldsymbol{r}) \approx \zeta_{\mathrm{AS}}(\boldsymbol{r})\exp(-i\boldsymbol{k}_{\mathrm{AS}} \cdot \boldsymbol{r}_i)$, with $\zeta_{\mathrm{AS}}(\boldsymbol{r}) = \frac{\varepsilon_0}{z}\exp\left[ik_{\mathrm{AS}}\left(z+\frac{x^2+y^2}{2z}\right)\right]$ and $\boldsymbol{k}_{\mathrm{AS}} = k_{\mathrm{AS}}\hat{z}$ the wave vector of the detected anti-Stokes light. We approximate the detected anti-Stokes photon state by $|\gamma\rangle_i = \sqrt{p}\hat{a}_{\mathrm{AS}}^{\dagger} e^{-i\boldsymbol{k}_S\cdot\boldsymbol{r}_i}|0\rangle_p$, where $\hat{a}_{\mathrm{AS}}^{\dagger}$ is a single-mode creation operator, and $p = \frac{\Omega_W^2}{\Delta^2}\Gamma T d\Omega \ll 1$ is the small probability for one atom to scatter one Stokes photon into the detection solid angle $d\Omega$. Substituting $|\gamma\rangle_{\mathrm{i}}$ into Eq. (A.4) we obtain $|\psi\rangle \approx 1 + \sqrt{p}\left(\sum_{i=1}^{N} e^{i\Delta\boldsymbol{k}\cdot\boldsymbol{r}_i}\sigma_{ba}^{i}\right)\hat{a}_{\mathrm{AS}}^{\dagger}|vac\rangle$, where $\Delta\boldsymbol{k} = \boldsymbol{k}_W - \boldsymbol{k}_{\mathrm{AS}}$ is the momentum difference between the write light and the Stokes mode. Defining a bosonic collective-state operator $S^{\dagger} = \frac{1}{\sqrt{N}}\sum_{i=1}^{N} e^{i\Delta\boldsymbol{k}\cdot\boldsymbol{r}_i}\sigma_{ba}^{i}$, we have $[S, S^{\dagger}] \approx 1$. The atom-light system is described by $|\psi\rangle \approx 1 + \sqrt{\chi}S^{\dagger}\hat{a}_{\mathrm{AS}}^{\dagger}|vac\rangle$, with $\chi = Np$ the probability to detect one Stokes photon in write process. It is easily seen that when an anti-Stokes photon is detected, the atomic ensemble is projected into the collective excited state, or in other words a spin wave is imprinted into the atomic ensemble. The conventional single-mode condition that $F = \frac{A}{\lambda L} \approx 1$ where F is the Fresnel number, $A = \pi W_a^2$, the cross-section area can be obtained by setting the two diffraction angles θ_{W_a} and θ_L are equal. In this case, the detection solid angle can be approximated by λ^2/A. Then we have

the total excitation probability $\chi = \frac{\Omega_W^2}{\Delta^2} N\Gamma T \frac{\lambda^2}{A} \sim d_0 \Gamma' T$, where $d_0 = N\sigma_0/A$ with $\sigma_0 = \frac{\lambda^2}{2\pi}$. To ensure we are in the spontaneous Raman scattering regime, we require the excitation probability $\chi \ll 1$. Note that in write process, there is no constructive interference in the forward direction, because when one atom scattering an anti-Stokes photon, it changes to another ground state $|b\rangle$ and thus all the terms in Eq. (A.4) are orthogonal to each other.

B Read Process

In the read process, a strong classical read light is applied to the atomic ensemble to convert the collective excitation into a Stokes photon. The weak Stokes field and the strong read light satisfy the EIT condition [19,20], and thus the Stokes field is not absorbed by the atoms in ground state $|a\rangle$.

Assume the strong classical read light coupling the excited state $|e\rangle$ and $|b\rangle$ ground state is counter-propagating with the write light $\boldsymbol{k}_\mathrm{R} = -k_\mathrm{R}\hat{z}$. The atom in state $|b\rangle$ is excited by the read light and transferred back to ground state $|a\rangle$ generating an anti-Stokes photon simultaneously. In contrast to the write process, the light emitted from different atoms will interfere with each other, and constructive interference occurs in the direction where mode-match condition is satisfied. The read process can be described by $\frac{1}{\sqrt{N}} \sum_{i=1}^{N} e^{i\Delta \boldsymbol{k}\cdot \boldsymbol{r}_i} |a \ldots b_i \ldots a\rangle \Rightarrow \otimes_i |a\rangle_i E_S(\boldsymbol{r}')$. The spatial wave function of the Stokes field on the observation point can be expressed as

$$E_S(\boldsymbol{r}') = \frac{1}{\sqrt{N}} \sum_{i=1}^{N} e^{i(\Delta \boldsymbol{k}+\boldsymbol{k}_R)\cdot \boldsymbol{r}_i} \frac{\varepsilon_0}{\Delta r_i'} e^{ik_S \Delta r_i'} \tag{B.1}$$

with $\Delta r_i' = |\boldsymbol{r}' - \boldsymbol{r}_i|$, where the atoms are treated as point light sources. Assume we observe Stokes light along the backward direction. Under the paraxial approximation, we can write the Stokes light as

$$\begin{aligned} E_S(\boldsymbol{r}') \sim \frac{1}{\sqrt{N}} \sum_{i=1}^{N} & e^{i(\Delta \boldsymbol{k}+\boldsymbol{k}_R)\cdot \boldsymbol{r}_i} \frac{\varepsilon_0}{|z' - z_i|} e^{-ik_S \cdot \boldsymbol{r}_i} \\ & \times \exp\left[ik_S \left(|z'| + \frac{x_i^2 + y_i^2}{2|z' - z_i|} + \frac{x'^2 + y'^2}{2|z' - z_i|} \right.\right. \\ & \left.\left. - \frac{x_i x' + y_i y'}{|z' - z_i|} \right) \right]. \end{aligned} \tag{B.2}$$

It can be readily seen that the once the mode-match condition $\boldsymbol{k}_W - \boldsymbol{k}_\mathrm{AS} + \boldsymbol{k}_\mathrm{R} - \boldsymbol{k}_\mathrm{S} = 0$ is satisfied, constructive interference will be observed on the detection surface. The Stokes field can be described by $E_\mathrm{S}(\boldsymbol{r}') \approx \sqrt{N} \int d\boldsymbol{r}'' n(\mathbf{r}'') \zeta_\mathrm{S}(\boldsymbol{r}') = \sqrt{N} \zeta_\mathrm{S}(\boldsymbol{r}')$ where $\zeta_\mathrm{S}(\boldsymbol{r}') = \frac{\varepsilon_0}{z'} \exp\left[-\mathrm{i} k_\mathrm{S} \left(z' + \frac{x'^2 + y'^2}{2z'} \right) \right]$ and $n(\mathbf{r})$ is atomic density distribution, and we have assumed the detection angle $\theta' \leq \min(\theta_{W_a}, \theta_L)$.

One can see that the intensity of the Stokes light is proportional to the atomic number N and the detection solid angle. The retrieval efficiency can be estimated by $\eta_{\text{ret}} \sim \frac{\Gamma N d\Omega}{\Gamma N d\Omega + \Gamma} = \frac{N d\Omega}{N d\Omega + 1}$, where N is the number of atoms, and $d\Omega$ is the solid angle in which we have constructive interference. Under the single-mode condition $d\Omega \sim \frac{\lambda^2}{A}$, a direct calculation shows that the retrieval efficiency $\eta_{\text{ret}} \sim 1 - \frac{1}{d_0}$ is given by the optical depth d_0. Note that taking into account the narrow EIT window, the error in retrieval efficiency scales as $\frac{1}{\sqrt{d_0}}$ [47].

The Stokes field couples the excited state and ground state, while it will not be absorbed since the atom-light system fulfills the EIT condition. In this case the Stokes light propagates in the atomic ensemble slower than the read light. Thus we require the read light pulse is sufficiently long so that all the anti-Stokes light can propagate out of the atomic ensemble.

The read process can be described using the dark-state polariton theory [19,20]. The read light may be described by $\boldsymbol{E}_{\text{R}}(\boldsymbol{r},t) = \hat{\epsilon}_{\text{R}} E_{\text{R}}(\boldsymbol{r},t) e^{i(\boldsymbol{k}_{\text{R}} \cdot \boldsymbol{r} - \omega_{\text{R}} t)} +$ h.c., where $\hat{\epsilon}_{\text{R}}$ is the polarization unit vector, $\omega_R = ck_R$ is the frequency of the write light. The Stokes field is approximated by a single-mode light $\boldsymbol{E}_S(\boldsymbol{r},t) = \hat{\epsilon_S} \hat{a}_S e^{i(\boldsymbol{k}_S \cdot \boldsymbol{r} - \omega_S t)} +$ h.c. The Hamiltonian describing the read process is given by $H = \sum_{i=1}^{N} [-\hbar \Omega_R(\text{t}) e^{i(\boldsymbol{k}_{\text{R}} \cdot \boldsymbol{r}_i - \omega_R t)} \sigma_{\text{eb}}^i + \hbar g_S \hat{a}_S e^{i(\boldsymbol{k}_S \cdot \boldsymbol{r}_i - \omega_S t)} \sigma_{\text{ea}}^i] +$h. c. with Ω_R the Rabi frequency of the read light and g_S the coupling coefficient, where we have assumed single-photon and two-photon resonance are both satisfied. This Hamiltonian has a series of adiabatic eigenstates with vanishing excited state component, i.e. a dark-state polariton. The simplest dark-state polariton can be described by $|D,1\rangle = \left(cos\theta \hat{a}_S^\dagger - sin\theta S'^\dagger\right)|vac\rangle$, where $tan\theta = \frac{g\sqrt{N}}{\Omega_R(t)}$ and $S'^\dagger = \frac{1}{\sqrt{N}} \sum_{i=1}^{N} e^{i\Delta \boldsymbol{k}' \cdot \boldsymbol{r}_i} \sigma_{\text{ba}}^i$ with $\Delta \boldsymbol{k}' = \boldsymbol{k}_R - \boldsymbol{k}_S$. If the Rabi frequency adiabatically changes from 0 to a large value, θ will vary from $\pi/2$ to 0. Consequently, the dark-state polariton will change from the collective excited state to the ground state and simultaneously emit a Stokes photon. Therefore, if the collective state imprinted in the write process $S^\dagger|vac\rangle$ is the same as the collective state $S'^\dagger|vac\rangle$ which can be fully retrieved out during the read process, the retrieve efficiency will reach the maximum. Again we obtain the mode-match condition $\boldsymbol{k}_{\text{W}} - \boldsymbol{k}_{\text{AS}} + \boldsymbol{k}_{\text{R}} - \boldsymbol{k}_{\text{S}} = 0$.

After the retrieval process, the whole state of anti-Stokes and Stokes photons can be expressed as $|\psi\rangle \approx 1 + \sqrt{\chi} \hat{a}_{\text{AS}}^\dagger \hat{a}_S^\dagger vac\rangle$. It can be easily seen that once there is a photon detected in the anti-Stokes field with a probability of χ, we can obtain a Stokes photon with certainty. In the discussion above, we only expand the perturbation theory to the first order. Taking into account higher-order excitations, the whole state of Stokes and anti-Stokes field may be described a two-mode squeezed state with excitation probability $\chi \ll 1$.

REFERENCES

[1] C.H. Bennett and G. Brassard, in Proceedings of the IEEE International Conference on Computers, systems, and signal processing, IEEE, Bangalore, India, New York (1984).

[2] N. Gisin, G. Ribordy, W. Tittel, and H. Zbinden, "Quantum Cryptography," Rev. Mod. Phys. 74, 145 (2002).
[3] E. Knill, R. Laflamme, and G.J. Milburn, "A Scheme for Efficient Quantum Computation with Linear Optics," Nature 409, 46–52 (2001).
[4] D. Browne and T. Rudolph, "Resource-Efficient Linear Optical Quantum Computation," Phys. Rev. Lett. 95, 010501 (2005).
[5] P. Michler, A. Kiraz, C. Becher, W. Schoenfeld, P. Petroff, L.D. Zhang, E. Hu, and A. Imamoglu, "A Quantum Dot Single-Photon Turnstile Device," Science 290, 2282–2285 (2000).
[6] C. Santori, M. Pelton, G. Solomon, Y. Dale, and Y. Yamamoto, "Triggered Single Photons from a Quantum Dot," Phys. Rev. Lett. 86, 1502–1505 (2001).
[7] A. Kuhn, M. Hennrich, and G. Rempe, "Deterministic Single-Photon Source for Distributed Quantum Networking," Phys. Rev. Lett. 89, 067901 (2002).
[8] J. McKeever, A. Boca, A. Boozer, R. Miller, J. Buck, A. Kuzmich, and H. Kimble, "Deterministic Generation of Single Photons from One Atom Trapped in a Cavity," Science 303, 1992–1994 (2004).
[9] C. Kurtsiefer, S. Mayer, P. Zarda, and H. Weinfurter, "Stable Solid-State Source of Single Photons," Phys. Rev. Lett. 85, 290–293 (2000).
[10] L.-M. Duan, M.D. Lukin, J.I. Cirac, and P. Zoller, "Long-Distance Quantum Communication with Atomic Ensembles and Linear Optics," Nature 414, 413–418 (2001).
[11] P. Kok, W.J. Munro, K. Nemoto, T.C. Ralph, J.P. Dowling, and G.J. Milburn, "Linear Optical Quantum Computing with Photonic Qubits," Rev. Mod. Phys. 79, 135–174 (2007).
[12] J.-W. Pan, Z.-B. Chen, C.-Y. Lu, M. Zukowski, H. Weinfurter, and A. Zeilinger, "Multi-Photon Entanglement and Interferometry," Rev. Mod. Phys. 84, 777–838 (2012).
[13] C.-W. Chou, S.V. Polyakov, A. Kuzmich, and H.J. Kimble, "Single-Photon Generation from Stored Excitation in an Atomic Ensemble," Phys. Rev. Lett. 92, 213601 (2004).
[14] T. Chaneliere, D.N. Matsukevich, S.D. Jenkins, S.-Y. Lan, T.A.B. Kennedy, and A. Kuzmich, "Storage and Retrieval of Single Photons Transmitted Between Remote Quantum Memories," Nature 438, 833–836 (2005).
[15] M.D. Eisaman, A. Andre, F. Massou, M. Fleischhauer, A.S. Zibrov, and M.D. Lukin, "Electromagnetically Induced Transparency with Tunable Single-Photon Pulses," Nature 438, 837 (2005).
[16] Y.O. Dudin, L. Li, and A. Kuzmich, Phys. Rev. A 87, 031801(R) (2013).
[17] S. Chen, Y.-A. Chen, T. Strassel, Z.-S. Yuan, B. Zhao, J. Schmiedmayer, and J.-W. Pan, "Deterministic and Storable Single-Photon Source Based on a Quantum Memory," Phys. Rev. Lett. 97, 173004 (2006).
[18] D.N. Matsukevich, T. Chaneliere, S.D. Jenkins, S.-Y. Lan, T.A.B. Kennedy, and A. Kuzmich, "Deterministic Single Photons via Conditional Quantum Evolution," Phys. Rev. Lett. 97, 013601 (2006).
[19] M. Fleischhauer, A. Imamoglu, and J.P. Marangos, "Electromagnetically Induced Transparency: Optics in Coherent Media," Rev. Mod. Phys. 77, 633–673 (2005).
[20] M. Fleischhauer and M.D. Lukin, "Dark-State Polaritons in Electromagnetically Induced Transparency," Phys. Rev. Lett. 84, 5094–5097 (2000).
[21] D.F. Walls and G.J. Milburn, "Quantum Optics," Springer-Verlag, Heidelberg (1994).
[22] H.J. Metcalf and P. van der Straten, "Laser Cooling and Trapping," Springer-Verlag, New York (1999).
[23] S.V. Polyakov, C.W. Chou, D. Felinto, and H.J. Kimble, Phys. Rev. Lett. 93, 263601 (2004).
[24] P. Grangier, G. Roger, and A. Aspect, "Experimental Evidence for a Photon Anticorrelation Effect on a Beam Splitter: A New Light on Single-Photon Interferences," Europhys. Lett. 1, 173–179 (1986).
[25] C.K. Hong, Z.Y. Ou, and L. Mandel, "Measurement of Subpicosecond Time Intervals Between Two Photons by Interference," Phys. Rev. Lett. 59, 2044–2046 (1987).
[26] Z.Y. Ou, J.-K. Rhee, and L.J. Wang, "Photon Bunching and Multiphoton Interference in Parametric Down-Conversion," Phys. Rev. A 60, 593 (1999).
[27] T. Humble and W. Grice, "Effects of Spectral Entanglement in Polarization-Entanglement Swapping and Type-I Fusion Gates," Phys. Rev. A 77, 022312 (2008).

[28] Z.-S. Yuan, Y.-A. Chen, S. Chen, B. Zhao, M. Koch, T. Strassel, Y. Zhao, G.-J. Zhu, J. Schmiedmayer, and J.-W. Pan, "Synchronized Independent Narrow-Band Single Photons and Efficient Generation of Photonic Entanglement," Phys. Rev. Lett. 98, 180503 (2007).
[29] D. Felinto, C.W. Chou, J. Laurat, E.W. Schomburg, H. de Riedmatten, and H.J. Kimble, "Conditional Control of the Quantum States of Remote Atomic Memories for Quantum Networking," Nature Phys. 2, 844–848 (2006).
[30] T. Chaneliere, D.N. Matsukevich, S.D. Jenkins, S.-Y. Lan, R. Zhao, T.A.B. Kennedy, and A. Kuzmich, "Quantum Interference of Electromagnetic Fields from Remote Quantum Memories," Phys. Rev. Lett. 98, 113602 (2007).
[31] D.A. Braje, V. Balic, S. Goda, G.Y. Yin, and S.E. Harris, "Frequency Mixing Using Electromagnetically Induced Transparency in Cold Atoms," Phys. Rev. Lett. 93, 183601 (2004).
[32] P. Mosley, J.S. Lundeen, B.J. Smith, P. Wasylczyk, A.B. U'Ren, C. Silberhorn, and I.A. Walmsley, "Heralded Generation of Ultrafast Single Photons in Pure Quantum states," Phys. Rev. Lett. 100, 133601 (2008).
[33] Y.H. Shih and C.O. Alley, "New Type of Einstein-Podolsky-Rosen-Bohm Experiment Using Pairs of Light Quanta Produced by Optical Parametric Down Conversion," Phys. Rev. Lett. 61, 2921 (1988).
[34] J.F. Clauser, M. Horne, A. Shimony, and R.A. Holt, "Proposed Experiment to Test Local Hidden-Variable Theories," Phys. Rev. Lett. 23, 880 (1969).
[35] C.W. Chou, H. de Riedmatten, D. Felinto, S.V. Polyakov, S.J. van Enk, and H.J. Kimble, "Measurement-Induced Entanglement for Excitation Stored in Remote Atomic Ensembles," Nature 438, 828–832 (2005).
[36] C.W. Chou, J. Laurat, H. Deng, K.S. Choi, H. de Riedmatten, D. Felinto, and H.J. Kimble, "Functional Quantum Nodes for Entanglement Distribution over Scalable Quantum Networks," Science 316, 1316–1320 (2007).
[37] Z.S. Yuan, Y.A. Chen, B. Zhao, S. Chen, J. Schmiedmayer, and J.W. Pan, "Experimental Demonstration of a BDCZ Quantum Repeater Node," Nature 454, 1098–1101 (2008).
[38] K.S. Choi, H. Deng, J. Laurat, and H.J. Kimble, "Mapping Photonic Entanglement into and out of a Quantum Memory," Nature 452, 67–71 (2008).
[39] B. Zhao, Y.-A. Chen, X.-H. Bao, T. Strassel, C.-S. Chuu, X.-M. Jin, J. Schmiedmayer, Z.-S. Yuan, S. Chen, and J.-W. Pan, "A Millisecond Quantum Memory for Scalable Quantum Networks," Nature Phys. 5, 95–99 (2009).
[40] R. Zhao, Y.O. Dudin, S.D. Jenkins, C.J. Campbell, D.N. Matsukevich, T.A.B. Kennedy, and A. Kuzmich, "Long-Lived Quantum Memory," Nature Phys. 5, 100–104 (2009).
[41] A.G. Radnaev, Y.O. Dudin, R. Zhao, H.H. Jen, S.D. Jenkins, A. Kuzmich, and T.A.B. Kennedy, "A Quantum Memory with Telecom-Wavelength Conversion," Nature Phys. 6, 894–899 (2010).
[42] F. Yang, T. Mandel, C. Lutz, Z.-S. Yuan, and J.-W. Pan, "Transverse Mode Revival of a Light-Compensated Quantum Memory," Phys. Rev. A 83, 063420 (2011).
[43] J. Simon, H. Tanji, J.K. Thompson, and V. Vuletic, "Interfacing Collective Atomic Excitations and Single Photons," Phys. Rev. Lett. 98, 183601 (2007).
[44] X.H. Bao, A. Reingruber, P. Dietrich, J. Rui, A. Dück, T. Strassel, L. Li, N.L. Liu, B. Zhao, and J.W. Pan, "Efficient and Long-Lived Quantum Memory with Cold Atoms Inside a Ring Cavity," Nature Phys. 8, 517–521 (2012).
[45] M.G. Raymer and J. Mostowski, "Stimulated Raman Scattering: Unified Treatment of Spontaneous Initiation and Spatial Propagation," Phys. Rev. A 24, 1980–1993 (1981).
[46] M.O. Scully and M.S. Zubairy, "Quantum Qptics," Cambridge University Press (1997).
[47] A. Andre, "Nonclassical States of Light and Atomic Ensembles: Generation and New Applications," PhD Thesis, Harvard University, Graduate School of Arts and Sciences (2005).